Available online at www.sciencedirect.com
SCIENCE DIRECT
Journal of Solid State Chemistry 179 (2006) 1225–1229
JOURNAL OF SOLID STATE CHEMISTRY
www.elsevier.com/locate/jssc

Low temperature synthesis of Mn_3O_4 polyhedral nanocrystals and magnetic study

Li-Xia Yang[a,b], Ying-Jie Zhu[a,*], Hua Tong[a,b], Wei-Wei Wang[a,b], Guo-Feng Cheng[c]

[a]State Key Laboratory of High Performance Ceramics and Superfine Microstructure, Shanghai Institute of Ceramics, Chinese Academy of Sciences, Shanghai 200050, PR China
[b]Graduate School of Chinese Academy of Sciences, PR China
[c]Analysis & Testing Center for Inorganic Materials, Shanghai Institute of Ceramics, Chinese Academy of Sciences, Shanghai 200050, PR China

Received 30 November 2005; received in revised form 4 January 2006; accepted 16 January 2006
Available online 21 February 2006

Abstract

Manganese oxide (hausmannite) polyhedral nanocrystals were prepared by a microwave-assisted solution-based method using $Mn(CH_3COO)_2$ and $(CH_2)_6N_4$ at 80 °C. The as-prepared Mn_3O_4 nanocrystals were characterized by means of X-ray diffraction, field-emission transmission electron microscopy, field-emission scanning electron microscopy and Raman spectrum. Mn_3O_4 polyhedral nanocrystals prepared by microwave heating at 80 °C for 60 min were of cubic and rhombohedral shapes with the edge lengths in the range of 15–40 nm. Mn_3O_4 nanocrystals grew following the Ostwald ripening mechanism with increasing reaction time. High-resolution transmission electron microscopy and selected area electron diffraction confirm that the as-obtained polyhedral nanocrystals were single-crystalline. The magnetic behavior of Mn_3O_4 nanocrystals was studied. Mn_3O_4 nanocrystals show an obvious ferromagnetic behavior at low temperatures. The magnetic behavior of Mn_3O_4 nanocrystals was sensitive to crystal size. Ferromagnetic onset temperatures (T_c) of samples 1 and 3 are 40.6 and 41.1 K, respectively, lower than that observed for bulk Mn_3O_4 (42 K).

Keywords: Mn_3O_4; Nanocrystal; Chemical synthesis; Magnetic property

1. Introduction

Considerable research has recently focused on the synthesis of uniformly sized and shape-controlled nanoparticles of manganese oxides due to their potential applications in catalysis, high-density magnetic storage media, ion exchange, molecular adsorption and electronics [1–4], and hence on the study of physical and chemical properties related with the specific morphology. Among them, Mn_3O_4 (hausmannite) is known to be an efficient catalyst in some processes, such as the decomposition of waste gas NO_x, selective reduction of nitrobenzene or oxidation of methane and carbon monoxide [5–11]. Moreover, Mn_3O_4 is also used to produce soft magnetic materials such as manganese zinc ferrite [12]. Lithiation of Mn_3O_4 for synthesis of intercalation compounds such as lithium manganese oxides as electrode materials for rechargeable lithium batteries is now attracting a growing interest [13–15].

One of the keys to realization of these applications lies in synthesizing high-quality nanoparticles and thus studying the relationship between characteristics, size and morphology. This prompts scientists to continuously develop new physical and chemical preparation methods. Up to now, different methods have been developed to produce nanomaterials. Among them, solution-based methods have been recognized as an effective way in tailoring the morphology and properties of nanomaterials. In general, Mn_3O_4 powders were prepared by heating manganese oxides (e.g., MnO_2 and Mn_2O_3, etc.) or manganese hydroxides, oxyhydroxide, carbonate, nitrate and sulfate at about 1000 °C in air [16–19]. However, the calcination methods have a tendency to form hard solid with coarse grains. Another conventional process to synthesize Mn_3O_4 powders was solvothermal method, which usually involves

*Corresponding author. Fax: +86 21 52413122.
E-mail address: y.j.zhu@mail.sic.ac.cn (Y.-J. Zhu).

0022-4596/$ - see front matter © 2006 Elsevier Inc. All rights reserved.
doi:10.1016/j.jssc.2006.01.033

an organic solvent at higher reaction temperatures or for a long period of time [19,20]. More recently, Park et al. have reported the synthesis of monodisperse, size-controlled Mn_3O_4 nanoparticles by thermal decomposition of a single precursor $Mn(CH_3COO)_2$ in oleyamine under an inert atmosphere at 150–250 °C [21]. Ultrasonic irradiation was also used to synthesize Mn_3O_4 nanocrystallites employing the aqueous solution of manganese acetate without the addition of alkali [22]. Vázquez-Olmos et al. reported the synthesis of Mn_3O_4 nanorods using manganese acetate in a mixed solvents of *N,N′*-dimethylformamide and water at room temperature for 3 months [23]. Currently, developing a simple, low-temperature solution chemical synthetic method for shape-controlled Mn_3O_4 nanomaterials with a narrow size distribution is of great importance.

Herein, we report a facile route to prepare Mn_3O_4 polyhedral nanocrystals at low temperature via an aqueous solution containing $Mn(CH_3COO)_2$ and hexamethylenetetramine, the magnetic properties of Mn_3O_4 polyhedral nanocrystals have also been investigated. This method involves no seeds, catalysts, or templates and may be scaled up to synthesize Mn_3O_4 polyhedral nanocrystals on a large scale at relatively low cost.

2. Experimental details

2.1. Materials

$Mn(CH_3COO)_2 \cdot 4H_2O$ and $(CH_2)_6N_4$ (hexamethylenetetramine, HMT) were of analytical grade and used as received without further purification. Deionized water was used in all reactions.

2.2. Preparation of Mn_3O_4 nanocrystals

In a typical procedure, $Mn(CH_3COO)_2 \cdot 4H_2O$ (1 g) and HMT (1 g) were dissolved in 20 ml deionized water in a round-bottomed flask. Then, the solution was heated by microwave at 80 °C for 10 min (sample 1), 40 min (sample 2) and 60 min (sample 3), respectively. The microwave oven used was a focused single-mode microwave synthesis system equipped with a magnetic stirring (Discover, CEM, USA). The brown products were collected by centrifugation, washed with deionized water and absolute ethanol several times, and dried in air at 60 °C.

2.3. Characterization

X-ray powder diffraction (XRD) was performed with a Rigaku D/max 2550 V X-ray diffractometer with high-intensity Cu$K\alpha$ radiation ($\lambda = 1.54178$ Å) and a graphite monochromator. The morphology was studied by a field emission scanning electron microscopy (FESEM, JEOL, JSM-6700F) and field emission transmission electron microscope (TEM, JEOL, JEM-2100F). The Raman spectrum was taken at room temperature in the range of 200–900 cm^{-1} using a Dilor LabRam-1B Raman Spectrometer equipped with a CCD camera and an optical microscope that provided a laser beam. A red line (632.81 nm) was taken as a back-scattering source. The laser power in front of the microscope was 0.75 mW. The time for spectral acquisition was 50 s and each spectrum was recorded three times. Magnetic property data were collected with a quantum design physical property measurement system (PPMS). The magnetizations as a function of temperature in the range of 10–80 K with the magnetic field of 100 Oe were measured. The hysteresis loops were obtained at 10 K in a magnetic field that varied from +7 to −7 T.

3. Results and discussion

The crystallinity and phase of the products were examined by XRD. Fig. 1 shows the XRD patterns of samples 1 and 3. All the reflections of sample 1 can be indexed to a single tetragonal phase of Mn_3O_4, which is in good agreement with the reported data (JCPDS, 24-0734). No peaks from other phases are observed, which indicates a high purity of the obtained Mn_3O_4 product through the reaction of $Mn(CH_3COO)_2$ with HMT in an aqueous solution at 80 °C for 10 min. XRD pattern of sample 3 is similar to that of sample 1, indicating that the product was still a single phase of tetragonal Mn_3O_4 when prolonging the reaction time to 60 min.

Fig. 2 exhibits the Raman spectrum of sample 3. Three peaks at 658.4, 374.7 and 318.9 cm^{-1} were observed, in agreement with reported values for Mn_3O_4 [24–26], which further supports the XRD result. The peak at 658.4 cm^{-1} is characteristic of Mn_3O_4 with a spinel structure, similar result from Mn_3O_4 nanowires synthesized via an inverse microemulsion method was also reported [27].

Fig. 3 shows the representative TEM and FESEM micrographs of samples 1, 2 and 3. The effect of preparation time was studied in order to obtain a better

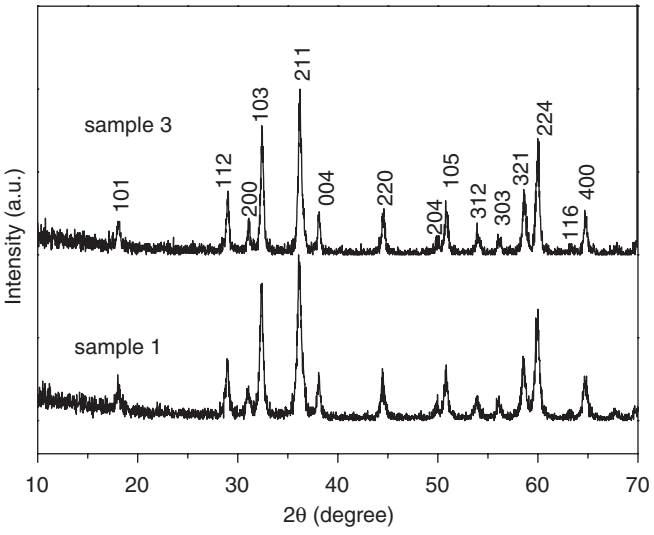

Fig. 1. XRD pattern of samples 1 and 3.

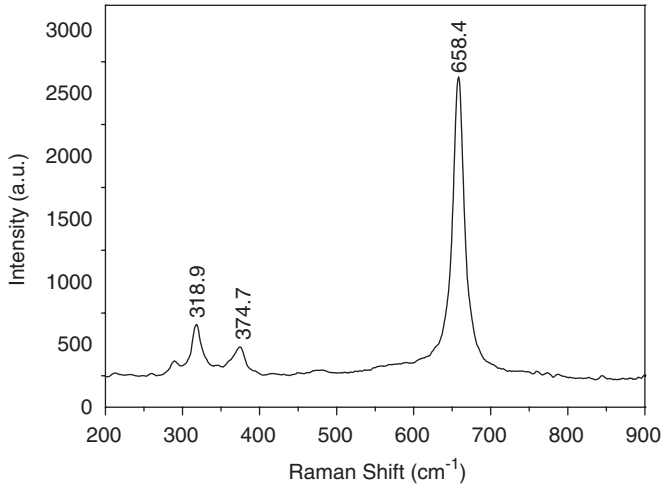

Fig. 2. Raman spectrum of Mn_3O_4 nanocrystals (sample 3).

understanding of the shape evolution of Mn_3O_4. At the early reaction stage (10 min), Mn_3O_4 nanocrystals were observed with multi-morphology, including cubes, ellipsoids and spherules. Most of the nanocrystals have sizes below 20 nm. The selected area electron diffraction pattern (SAED) shown in Fig. 3a exhibits multiple intense rings, which suggests that nanocrystals have no preferential orientation. When the temperature was prolonged to 40 min, it is evident that most nanocrystals have a cubic and rhombohedral shape with edge lengths up to 35 nm. A randomly chosen nanocrystal was given in Fig. 3c, which has a size ca. 35 nm. Shown in Fig. 3d is the corresponding high-resolution transmission electron microscopy (HRTEM) image and the corresponding SAED pattern. Like the XRD profile, the HRTEM image and the SAED pattern may also be indexed to tetragonal phase of Mn_3O_4. The observed lattice spacings of 0.485 and 0.282 nm correspond to the (101) and (200) planes of tetragonal Mn_3O_4, respectively. The SAED pattern taken along the $[1\bar{0}1]$ zone axis reveals that the nanocrystals are single-crystalline in nature. With the increase of reaction time to 60 min, more rhombohedral nanocrystals were observed. From the FESEM and TEM images in Fig. 3e and f, most of Mn_3O_4 nanocrystals are cubes and rhombohedra with edge lengths of 15–40 nm. The SAED pattern taken by focusing the incident electron beam along the [100] zone axis reveals a single crystalline structure. The observed lattice spacing of 0.486 nm corresponds to (101) plane of tetragonal Mn_3O_4. The visible lattice fringes further confirm that the as-obtained nanoparticles are single crystals.

The formation process of Mn_3O_4 nanocrystals may be explained as follows: firstly, OH^- ions formed as a result of decomposition of HMT, which provided a basic condition for nucleation. Subsequently, Mn_3O_4 nuclei formed rapidly, the reaction entered the crystal growth stage. Ostwald ripening made the larger nanocrystals grow at the expense of dissolving the smaller ones with increasing

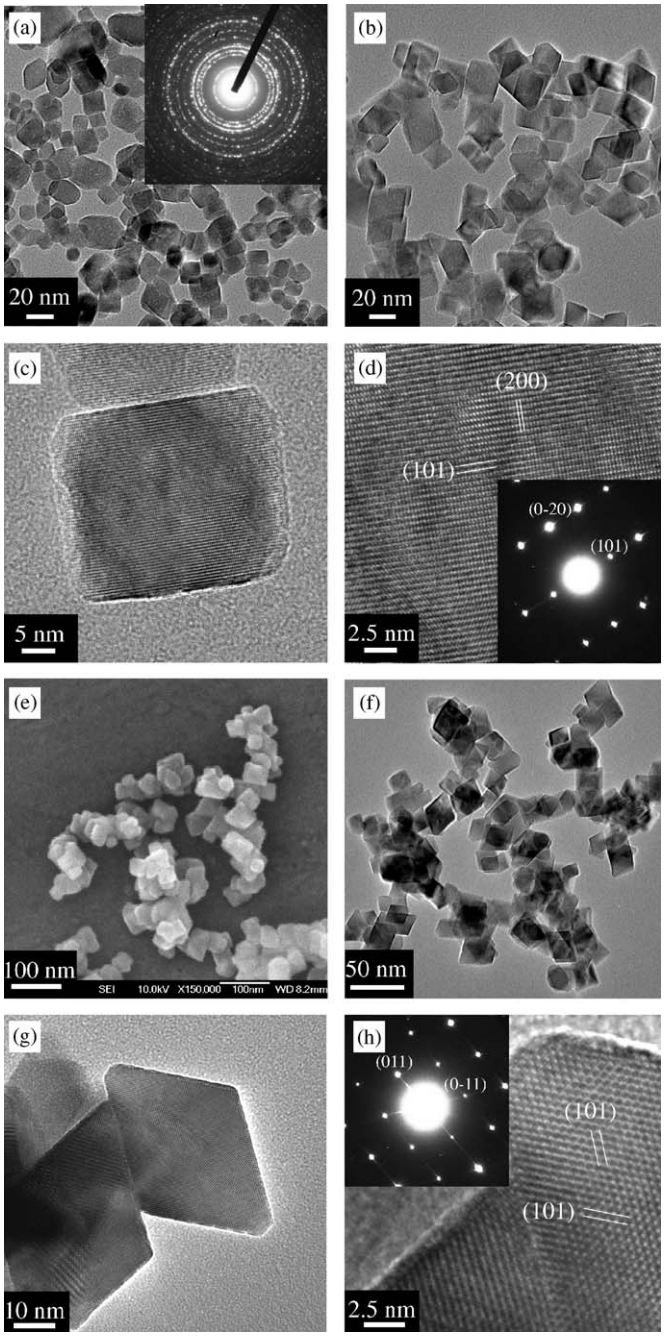

Fig. 3. TEM micrographs of Mn_3O_4 nanocrystals: (a) sample 1; (b) and (c) sample 2; (d) HRTEM image of an individual Mn_3O_4 nanocrystal (sample 2); (e) FESEM micrograph of Mn_3O_4 nanocrystals (sample 3); (f) and (g) TEM micrographs of Mn_3O_4 nanocrystals (sample 3); and (h) HRTEM image of an individual Mn_3O_4 nanocrystal (sample 3); the insets of (a), (d) and (h) show the corresponding SAED patterns.

reaction time, finally nanocrystals with polyhedral shape formed. The major chemical reactions for the formation of Mn_3O_4 nanocrystals in the aqueous solution can be summarized as follows:

$$(CH_2)_6N_4 + 6H_2O \rightarrow 4NH_3 + 6HCHO \quad (1)$$

$$NH_3 + H_2O \rightarrow NH_4^+ + OH^- \quad (2)$$

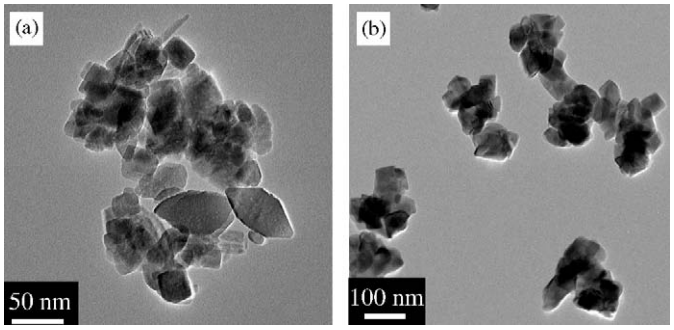

Fig. 4. TEM micrographs of different samples: (a) the sample prepared through the reaction of $Mn(CH_3COO)_2$ with HMT at room temperature for 6 h and (b) the sample prepared through the reaction of $MnCl_2$ with HMT at 80 °C for 10 min.

$$6Mn^{2+} + 12OH^- + O_2 \rightarrow 2Mn_3O_4 + 6H_2O \quad (3)$$

In fact, $Mn(CH_3COO)_2$ can react with HMT in aqueous solution to form Mn_3O_4 at room temperature, but it needs a longer period of time and the yield of the product is much less than that prepared by microwave heating at 80 °C for 10 min. TEM image of the product obtained at room temperature for 6 h given in Fig. 4a shows irregular nanoparticles with minor nanorods. Even when the reaction time was prolonged to 24 h, the shape remained almost the same. In addition, when $MnCl_2$ was introduced to replace $Mn(CH_3COO)_2$ as the divalent manganese source at 80 °C for 10 min, the products were severely agglomerated particles (Fig. 4b), also no polyhedral crystals were observed. In this case, we suggest that CH_3COO^- plays an important role in the formation of Mn_3O_4 polyhedral nanocrystals. The function of CH_3COO^- was discussed in the synthesis of MnOOH nanorods prepared by the hydrothermal route using $Mn_{12}O_{12}(RCOO)_{16}(H_2O)_n$ ($R = CH_3$, C_2H_5) at 150 °C for 24 h. The carboxylate ligands played the role of structuring agent in the synthesis and the increase of the electron donating capacity of the R groups favors the nanorods formation [28]. Vázquez-Olmos et al. suggested that there was a hydrolysis equilibrium of acetate anions in water, then OH^- formed [23]. The solution became more basic in the presence of acetate anions. Thus, Mn_3O_4 nanocrystals with a well-defined morphology were obtained.

The magnetic properties of Mn_3O_4 nanocrystals have been studied by measuring the magnetization as a function of temperature. Typical M–T curves of samples 1 and 3 are shown in Fig. 5, from which one can see that there is almost no change in the magnetization in the temperature range of 45–80 K, but increases sharply below 45 K. The two samples show an obvious ferromagnetic behavior. The value of magnetization reduces greatly with the decrease of the size, which is attributed to the increasing of surface to volume ratio, since the surface region leads to a decrease in the effective magnetic moment. The ferromagnetic onset temperatures (T_c) of samples 1 and 3 are 40.6 and 41.1 K, respectively, these two values are lower than that observed

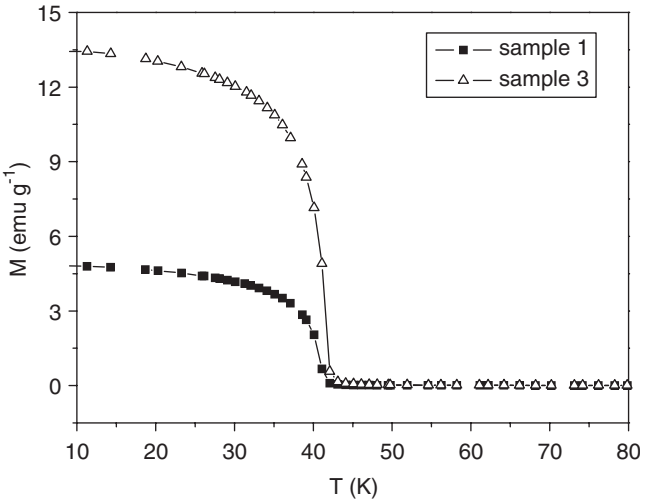

Fig. 5. Magnetization of Mn_3O_4 nanocrystals (samples 1 and 3) versus temperature.

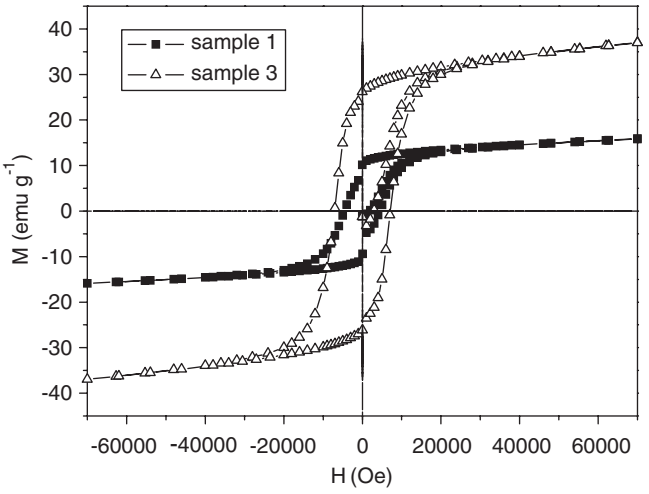

Fig. 6. Hysteresis loops of samples 1 and 3 at 10 K.

for bulk Mn_3O_4 (42 K) [29,30]. The T_c value decreases with decreasing size of the nanocrystals. Yu et al. reported T_c for nanoparticles prepared via vapor phase growth with diameters of 80, 40 and 25 nm are 44.3, 43.4 and 42.0 K, respectively [31]. In comparison, samples 1 and 3 with the sizes of nanocrystals below 40 nm show a lower T_c than those reported [31]. The hysteresis loops of samples 1 and 3 at 10 K were shown in Fig. 6. The maximum saturation magnetization (M_{max}) is about 15.9 and 37.0 emu/g for samples 1 and 3, respectively. Remanence ratios (M_r/M_{max}) of 0.64 and 0.71 were calculated from the remanence value (M_r) of 10.2 (sample 1) and 26.2 emu/g (sample 3). The coercivity (H_c) for samples 1 and 3 are 4496 and 7135 Oe, respectively.

4. Conclusion

In summary, we present a facile method for the preparation of Mn_3O_4 polyhedral nanocrystals through a microwave-assisted solution-based method using

$Mn(CH_3COO)_2$ and $(CH_2)_6N_4$ at 80 °C. It has been found that the Mn_3O_4 nanocrystals prepared at 80 °C for 60 min were of cubic and rhombohedral shapes and the edge lengths of these polyhedral nanocrystals were in the range of 15–40 nm. The growth of Mn_3O_4 nanocrystals follows the Ostwald ripening mechanism with the prolonging of reaction time. HRTEM and SAED pattern confirm that as-obtained nanocrystals are single crystals. Mn_3O_4 nanocrystals show an obvious ferromagnetic behavior at low temperatures. The magnetic behavior of Mn_3O_4 nanocrystals was sensitive to crystal size. The ferromagnetic onset temperatures (T_c) of samples 1 and 3 are 40.6 and 41.1 K, respectively, lower than that observed for bulk Mn_3O_4 (42 K).

Acknowledgments

Financial support from National Natural Science Foundation of China (50472014) and Chinese Academy of Sciences under the Program for Recruiting Outstanding Overseas Chinese (Hundred Talents Program) is gratefully acknowledged. We also thank the Fund for Innovation Research from Shanghai Institute of Ceramics, Chinese Academy of Sciences.

References

[1] A.R. Armstrong, P.G. Bruce, Nature 381 (1996) 499.
[2] Y.F. Shen, R.P. Zerger, R.N. Deguzman, S.I. Suib, L. Mccurdy, D.I. Potter, C.L. Oyoung, Science 260 (1993) 511.
[3] M.C. Bernard, H.L. Goff, B.V. Thi, J. Electrochem. Soc. 140 (1993) 3065.
[4] R. Jothiramalingam, B. Viswanathan, T.K. Varadarajan, Catal. Commun. 6 (2005) 41.
[5] T. Yamashita, A. Vannice, J. Catal. 163 (1996) 158.
[6] W.M. Wang, Y.N. Yang, J.Y. Zhang, Appl. Catal. A 133 (1995) 81.
[7] E. Grootendorst, Y. Verbeek, V. Ponce, J. Catal. 157 (1995) 706.
[8] L. Chen, T. Horiuchi, T. Mori, Appl. Catal. A: Gen. 209 (2001) 97.
[9] E.R. Stobhe, B.A.D. Boer, J.W. Geus, Catal. Today 47 (1999) 161.
[10] M.F.M. Zwinkels, S.G. Jaras, P.G. Menon, T.A. Griffin, Catal. Rev. Sci. Eng. 35 (1993) 319.
[11] Y. Lun, J. Yuan, P. Lin, Phys. Chem. Lett. 12 (1999) 82.
[12] V.V. Pankov, Ceram. Int. 14 (1988) 87.
[13] L. Sanchez, J. Farcy, J.-P. Pereira-Ramos, L. Hernan, J. Morales, J.L. Tirado, J. Mater. Chem. 6 (1996) 37.
[14] L. Sanchez, J.-P. Pereira-Ramos, Electrochim. Acta 42 (1997) 531.
[15] T. Kanasaku, K. Amezawa, N. Yamamoto, Solid State Ion. 133 (2000) 51.
[16] C.H. Shomate, J. Am. Chem. Soc. 65 (1943) 786.
[17] J.C. Southard, G.E. Moore, J. Am. Chem. Soc. 64 (1942) 1769.
[18] I. Ursu, R. Alexandrescu, I.N. Mihailescu, J. Phys. B 19 (1986) 825.
[19] Y.C. Zhang, T. Qiao, X.Y. Hu, J. Solid State Chem. 177 (2004) 4093.
[20] W.X. Zhang, Z.H. Yang, Y. Liu, S.P. Tang, X.Z. Han, M. Chen, J. Cryst. Growth 263 (2004) 394.
[21] W.S. Seo, H.H. Jo, K. Lee, B. Kim, S.J. Oh, J.T. Park, Angew. Chem. Int. Ed. 43 (2004) 1115.
[22] I.K. Gopalakrishnan, N. Bagkar, R. Ganguly, S.K. Kulshreshtha, J. Cryst. Growth 280 (2005) 436.
[23] A. Vázquez-Olmos, R. Redón, G. Rodríguez-Gattorno, M.E. Mata-Zamora, F. Morales-Leal, A.L. Fernández-Osorio, J.M. Saniger, J. Colloid Interface Sci. 291 (2005) 175.
[24] M.C. Bernard, A.H.L. Goff, B.V. Thi, J. Electrochem. Soc. 140 (1993) 3065.
[25] F. Buciuman, F. Patcas, R. Craciun, D.R.T. Zahn, Phys. Chem. Chem. Phys. 1 (1999) 185.
[26] F. Kapteijn, A.D. Van Langeveld, J.A. Moulijn, A. Andreini, M.A. Vuurman, A.M. Turek, J.-M. Jehng, I.E. Wachs, J. Catal. 150 (1994) 94.
[27] Y. Liu, Z. Liu, G. Wang, Appl. Phys. A 76 (2003) 1117.
[28] B. Folch, J. Larionova, Y. Guari, C. Guérin, C. Reibel, J. Solid State Chem. 178 (2005) 2368.
[29] G. Srinivasan, M.S. Seehra, Phys. Rev. B 28 (1983) 1.
[30] K. Dwight, N. Menyuk, Phys. Rev. 119 (1960) 1470.
[31] Y.Q. Chang, X.Y. Xu, X.H. Luo, C.P. Chen, D.P. Yu, J. Cryst. Growth 264 (2004) 232.